GALACTIC SURVEY AT 400 Mc/s BETWEEN DECLINATIONS −17° AND −49°

By R. X. McGee,* O. B. Slee,* and G. J. Stanley*

[*Manuscript received February* 16, 1955]

Summary

The zone of the sky between declinations −17° and −49° was surveyed with a pencil-beam aerial. The operating frequency was 400 Mc/s and the aerial beam width 2° between half-power points.

It is shown by means of contour diagrams of equivalent sky temperature that the central Milky Way consists of a narrow background of radiation (about 5° between half-power points) on which is superimposed a number of discrete radio sources. Test measurements at two points on the galactic plane indicate random polarization of the radiation.

A most intense source in R.A. 17 hr 42 min, Dec. −28·5° (1950) is believed to represent radiation from the galactic nucleus.

The radio-frequency spectra of the Milky Way sources and other sources observed in the course of the survey are shown to be divided into two classes, indicating two different mechanisms in the production of discrete source radiation.

I. Introduction

In general, surveys of galactic radio-frequency radiation have been deficient in important respects. On the one hand, wide-beam-aerial surveys have produced rather " smoothed out " contours of radio brightness, and on the other, interferometer surveys, while giving lists of many radio sources, have failed to show how these sources are associated with the background. Thus it has become obvious that improved methods such as pencil-beam surveys of high resolution, pioneered by Hanbury Brown and Hazard, are necessary before a balanced radio picture of the sky can be produced.

The present survey was undertaken to apply the pencil-beam technique to a sample of sky of outstanding interest, that region of the Milky Way in the direction of the galactic centre.

Reber (1944, 1948), Bolton and Westfold (1950), and others have shown that the contours of radio brightness ascend to a rather broad peak close to the calculated position of the galactic centre. Bolton *et al.* (1954), using two types of interferometer and a 6° pencil beam in the Scorpio-Sagittarius region, resolved the broad radio maximum into two large extended sources. One of these which they call " source L " corresponds approximately in position to the intense discrete source discovered by Piddington and Minnett (1951) at a frequency of 1210 Mc/s and inferred to be an extended physical object in the direction of the centre of the galaxy. Mills (1952) and Bolton, Stanley, and Slee (1954) observed

* Division of Radiophysics, C.S.I.R.O., University Grounds, Sydney.

this object as a discrete source with interferometers at 100 Mc/s, but it was pointed out by Bolton *et al.* (1954) that the central Milky Way region is rather unsuitable for the use of interferometers of moderately broad primary beam owing to the confusion caused by a number of sources in such a beam at the same time. The present work clears up this confusion to a large extent and indicates considerable detail in the fine structure of the Milky Way.

The survey was carried out over the zone of the sky between declinations −17° and −49°. The operating frequency was 400 Mc/s, and the angular width of the aerial beam was 2° between half-power points. A preliminary report of the observations on the region surrounding the galactic centre, which lead to the recognition that an intense observed source may well be the galactic nucleus itself, has been presented elsewhere by McGee and Bolton (1954).

The present paper begins with a short description of the aerial and receiver used. Following is a discussion of the method of calibrating the equipment in order to establish absolute values for observed temperatures so that contours of equivalent sky temperatures could in turn be drawn. Results of the survey of the central Milky Way are then summarized, with emphasis placed on the " galactic nucleus source ". The radiation in this region consists of a general background on which are superimposed several radio sources, and tests at two points on the galactic plane indicate random polarization of the radiation. Finally, a list of discrete sources is presented and the more important ones and the trends of the spectra discussed. It is shown that the spectra may be divided into two classes, some displaying the usual non-thermal type of emission and others suggesting thermal emission from a gas cloud over part of the frequency range.

II. Aerial and Receiver

(*a*) *The Aerial*

The reflector was a paraboloid of revolution of aperture 80 ft and focal length 40 ft set with its axis vertical. The aerial beam width was 2° at 400 Mc/s, and the beam could be directed by tilting the mast supporting the feed. The reflector was hollowed out of the sandy soil at the Dover Heights field station to a maximum depth of approximately 9 ft. The surface was then consolidated with concrete and completely covered with wire netting of ½-in. mesh and an additional supporting structure was added above ground level to give the full 80-ft diameter. Overall surface accuracy was maintained to within 1 in. The reflector was available for use at any desired plane of polarization of the primary feed. A photograph of the aerial is shown in Plate 1.

The primary aerial consisted of a conical dipole and plane reflector, a quarter-wavelength apart, fed by means of a shielded twin-wire transmission line. The shield and aerial were supported by a 3-in. aluminium mast guyed with nylon parachute cord, a material chosen to eliminate the possibility of spurious lobes in the aerial pattern.

The mast was pivoted and counterweighted on a 3-ft frame in the centre of the reflector in such a way that the feed could be tilted in the meridian plane by adjustment of the north and south guys. The relation between the angle of

tilt of the mast and the zenith angle of the direction of maximum sensitivity of the aerial beam was determined experimentally at a number of points by observations of the radio star Centaurus-A and of the Sun as it approached the summer solstice. The method of tilting the feed to alter the direction of the aerial beam has been fully described by Brown and Hazard (1951) and Silver and Pao (1944). The experimental ratio between the angle of tilt and the zenith angle of the beam was found to be very close to $-0{\cdot}92$, given in the latter reference, even up to angles of 20°. For a 2° beam it was possible to observe at angular distances up to 15° on either side of the zenith without serious distortion in aerial beam shape or appreciable loss in power gain.* Silver and Pao's relation between relative gain and angle of tilt was well verified by the solar observations.

The actual setting of the mast was done with the aid of a theodolite so that in the mechanical positioning of the beam high accuracy was obtained.

(*b*) *The Aerial Power Diagram*

The usual method of obtaining a diagram of power directivity of a large aerial of this type is to allow a well-established and isolated celestial point source to trace out the diagram as it passes through the beam. Since there was unfortunately no simple point source available in the zone under survey by this aerial, observations on two objects of angular width comparable with the beam width were used indirectly to confirm calculations. These were the radio source Centaurus-A, which has been found to be a combination of point source and associated spread source, and the Sun, whose dimensions at 400 Mc/s are fairly accurately known.

The primary field diagram was obtained by careful measurement. The secondary aerial power pattern was then calculated using the relation derived from a well-known formula (e.g. Slater 1942, p. 258)

$$F=2\pi\int_0^R rf(r)J_0(\beta r)\mathrm{d}r,$$

where F is the relative power, R is the radius of the aperture of the paraboloid, r is the radial distance, $\beta=(2\pi/\lambda)(\frac{1}{2}\pi-\theta)$, θ being measured from the zenith, and $\mathrm{f}(r)$ represents the primary field in the aperture plane.

It will be seen that radial symmetry is inferred. Corresponding values of primary field in the E and H planes were so close to one another that a mean curve, $\mathrm{f}(r)$, was taken as a very good approximation to the primary field.

The width of the aerial beam between half-power points was $2{\cdot}1\pm0{\cdot}1°$.

Observations made on Centaurus-A with several different orientations of the feed showed that the assumption of radial symmetry was justified.

* *Note added in Proof.*—Recently the diffraction theory of coma has been applied to the aerial in a semi-quantitative way and this aberration was seen to be more serious than had been indicated by geometrical optics. It is believed that such effects as the " bulges " at declinations —21° and —45° in the 50 °K contour on the left-hand side of Figure 2, the appearance of source No. 9, and the low level contours in Figure 5 may be attributed to third order coma.

(c) *The Receiver*

The observations were made using a Dicke type 25 c/s electronic radio-frequency switch which connected a conventional superheterodyne receiver alternately to the aerial and to a reference resistor at ambient temperature. The receiver output was applied to a synchronous detector, and the noise temperature difference was indicated on a recording ammeter. This method ensures that receiver gain fluctuations have little effect on the stability of the system.

The receiver noise factor was 11. The average receiver noise fluctuations represented an equivalent temperature of 2–3 °K at all aerial temperatures.

III. Calibration of the Equipment

In calibrating the equipment the aim was to extract equivalent sky temperatures from the observed temperatures. Firstly, it was necessary to obtain a scale factor which would refer all observations to a common temperature scale. The method used is discussed in Section III (*a*).

The equivalent temperature measured at the receiver input terminals includes contributions from the ground surrounding the reflector and from the aerial feeder as well as from the sky in the aerial beam. The derivation of an expression for sky temperature T_s is given in Section III (*b*), and in Section III (*c*) there follows an estimation of the ground contribution T_g. The effects caused by loss in the feeder may be measured directly.

(a) *Relative Temperature Calibration*

The scale factor was obtained by daily measurements of Centaurus-A, and then all observed deflections were referred to the deflection produced by Centaurus-A.

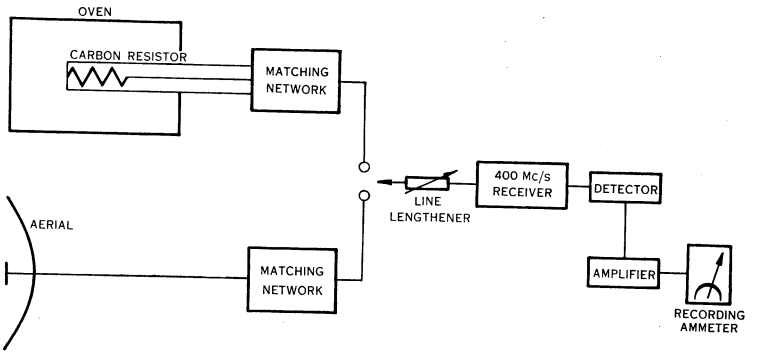

Fig. 1.—Block diagram of calibration equipment for 400 Mc/s receiving equipment.

The observed intensity of this calibrating source was then converted to an equivalent temperature by replacement of the aerial by a thermal load which could be cooled or heated over a temperature range extending from 75 °K below to 70 °K above ambient temperature. Figure 1 indicates the experimental arrangement for these measurements. The matching network of two variables

ensured that the thermal load, a carbon resistor of good high frequency characteristics mounted in a coaxial line, was very well matched to the receiver. This condition was continuously checked by the line lengthener in series with the receiver. Satisfactory matching conditions were assumed to exist when the cyclic deflections, occurring on the recording ammeter as the line lengthener was varied through a wavelength, were no longer visible above the receiver noise fluctuations. This is several orders of magnitude better than the best matching conditions indicated by the slotted line devices available on the field station.

The detector law and gain of the post-detector amplifier were checked by a carefully matched noise generator, and the recorder deflections were found to be proportional within required accuracy to power and hence to equivalent temperature over the full range of observed temperatures.

It was deduced from the measurements that the radiation from Centaurus-A at 400 Mc/s was equivalent to an aerial temperature of 74 ± 6 °K above that of the cold sky in its immediate vicinity. This value having been determined, all observed recorder deflections could be expressed in relative temperature units.

(b) The Equivalent Sky Temperature

In any observation, the equivalent aerial temperature T_a is made up of the integrated beam temperature T_s, due to the radiation directed to the primary aerial by the reflector, and the unwanted ground contribution T_g resulting from thermal emission at ambient temperature, and such sky emission as may be reflected from the ground into the primary pattern.

$$T_a = T_s + T_g. \quad \ldots\ldots\ldots\ldots\ldots\ldots \quad (1)$$

Note that if the temperature of the sky is constant over the solid angle subtended by the secondary power diagram of the aerial, T_s may be called the equivalent sky temperature.

The quantity which can be measured directly is the equivalent temperature at the receiver input, T_r. It is different from T_a because of loss in the feeder. The aerial itself is regarded as a lossless element and of the power delivered from the aerial, $\alpha[kT_a\Delta f]$ arrives at the receiver input terminals and $(1-\alpha)[kT_a\Delta f]$ is absorbed in the feeder. The feeder is at ambient temperature, T_0, and so contributes a power $(1-\alpha)[kT_0\Delta f]$ at the receiver input. Therefore, the power delivered to the receiver is

$$k\Delta f\{\alpha T_a + (1-\alpha)T_0\},$$

where α represents the effect of power losses in the aerial feeder, k is Boltzmann's constant, and Δf is the bandwidth. For this discussion we write the expression in terms of temperatures

$$T_r = \alpha T_a + (1-\alpha)T_0. \quad \ldots\ldots\ldots\ldots\ldots\ldots \quad (2)$$

Therefore, from equations (1) and (2), the required equivalent sky temperature T_s is

$$T_s = \frac{T_r - (1-\alpha)T_0}{\alpha} - T_g. \quad \ldots\ldots\ldots\ldots\ldots \quad (3)$$

α is obtained by measurement, T_g is estimated as in Section III (*c*), and so T_s may be calculated.

(c) *Estimation of the Ground Contribution*, T_g

An unwanted contribution to the observed aerial temperature occurred because the pattern of the power directivity of the primary aerial extended beyond the limits of the paraboloid aperture and over the surrounding terrain. This temperature T_g consists of a small component due to any sky radiation reflected from the ground and the main temperature T_g', say, due to thermal emission from the ground at ambient temperature.

For the calculation of T_g', we first assume flat ground conditions and later try to correct for the irregularities and changes in the terrain. In general,

$$T_g' = T_0 \frac{\int_{\theta}^{\pi} \int_{0}^{2\pi} A(\theta, \varphi) P(\theta, \varphi) \sin\theta \, d\theta \, d\varphi}{\int_{0}^{\pi} \int_{0}^{2\pi} P(\theta, \varphi) \sin\theta \, d\theta \, d\varphi}, \quad \ldots\ldots\ldots \quad (4)$$

where $P(\theta, \varphi)$ is the power diagram of the primary aerial, $A(\theta, \varphi)$ is the power absorption coefficient of the surrounding medium, and θ is the angle subtended at the feed by a radius of the reflector aperture. The method used to integrate equation (4) is given in Appendix I.

In order to calculate the absorption coefficient $A(\theta, \varphi)$ it was necessary to know the dielectric constant and conductivity of the soil. These constants were kindly measured on a number of representative samples by Dr. J. S. Dryden of the Division of Electrotechnology, C.S.I.R.O. The values found were dielectric constant 4 and conductivity 1×10^{-4} mhos per metre.

Evaluation of equation (4) made $T_g' = 0 \cdot 095 \, T_0$. Corrections were then applied to take into account departures from flat ground conditions. For example, the aerial is situated quite close to the cliff edge and approximately one-sixth of the effective spillover area extends over sea-water supplying a negligible contribution at ambient temperature and a small contribution from the reflected sky radiation. It is estimated that the equivalent temperature from reflected radiation from both sea and soil was only $0 \cdot 5$ °K in the cases used here. The low vegetation in places was considered to cause only second order effects at this frequency.

The value of T_g obtained when the region of lowest sky temperature was observed with the aerial in the zenith position was 22 °K. The errors involved in this estimate amount to probably ± 20 per cent.

Further measurements were made to check on the extent of change that could be expected in T_g as the mast was tilted, but the overall effect was well within the limits quoted above.

IV. Absolute Temperatures at Some Positions in the Sky

(a) *Observation of the Minimum Temperature of the Cold Sky*

The cold sky, i.e. regions away from the galactic plane and the discrete sources, exhibited such slow changes of temperature that it was not considered worth while to draw contours.

Brightness contours in previous surveys, e.g. Bolton and Westfold (1950), indicate that there is a large region of minimum sky temperature in the

approximate vicinity of the south galactic pole. Since the centre of this region sweeps through the zenith position of the aerial beam it was chosen as the first point for absolute measurement.

The equipment was set up in the same manner as shown in Figure 1. Interchanges between the aerial and the calibrating resistor at ambient temperature were made every 10 min over a 2-hr period. The deflections on the recorder chart indicating the differences between sky and ambient temperatures were constant to less than 2 per cent. over all measurements. The relative calibration by heating and cooling the resistor was then repeated. T_0 remained at 285 °K throughout and the observed value of T_r, the equivalent temperature at the receiver input, was 90 ± 6 °K.

The power loss factor α, measured for both aerial feeder and matching network by two independent methods, had a value $0 \cdot 77 \pm 0 \cdot 04$ which was in good agreement with the calculated value.

Substitution in equation (2) for T_r, α, T_0, and T_g resulted in an equivalent sky temperature of 10 ± 5 °K (p.e.) at 400 Mc/s for the cold region whose central position was R.A. 04 hr 30 min, Dec. $-33 \cdot 9°$.

(b) Observations along the Base Level of the Milky Way Contours

The same technique was applied at positions that gave an absolute calibration for the lowest level contour drawn in the diagrams of the radio Milky Way. The positions and temperature are given in Section V (*a*).

V. Survey of the Milky Way

The main effort in this survey was concentrated on the Milky Way in the zone of declinations from $-17°$ to $-49°$. After the daily calibrating observation of Centaurus-A the aerial beam was directed towards the region of the sky under investigation. Checks were made from time to time to make sure that the position of the mast did not change due to the effects of varying weather conditions on the nylon guys; under the worst observing conditions the maximum movement of the dipole was held to $0 \cdot 1°$.

The Milky Way was observed on one fixed declination per day, changes in Right Ascension occurring as the rotation of the Earth swept the aerial beam across the sky. In a preliminary survey observations were made at intervals of 1° in declination. Later, in order to cover the more interesting regions in greater detail, intervals of $\frac{1}{2}°$ were used. The record obtained on a particular declination was repeated until features of the variation of equivalent temperature with sidereal time were either satisfactorily reproduced or revealed as spurious and discarded.

For the analysis and fitting together of the 50 or so individual records the adopted unit of intensity was the deflection produced by Centaurus-A above a level through points on its observed temperature curve separated by 20 min in sidereal time. This level was selected since it was well above the complications in recorded pattern caused by the spread object which forms part of Centaurus-A, and thus errors which could arise in deciding a true base line for the source were

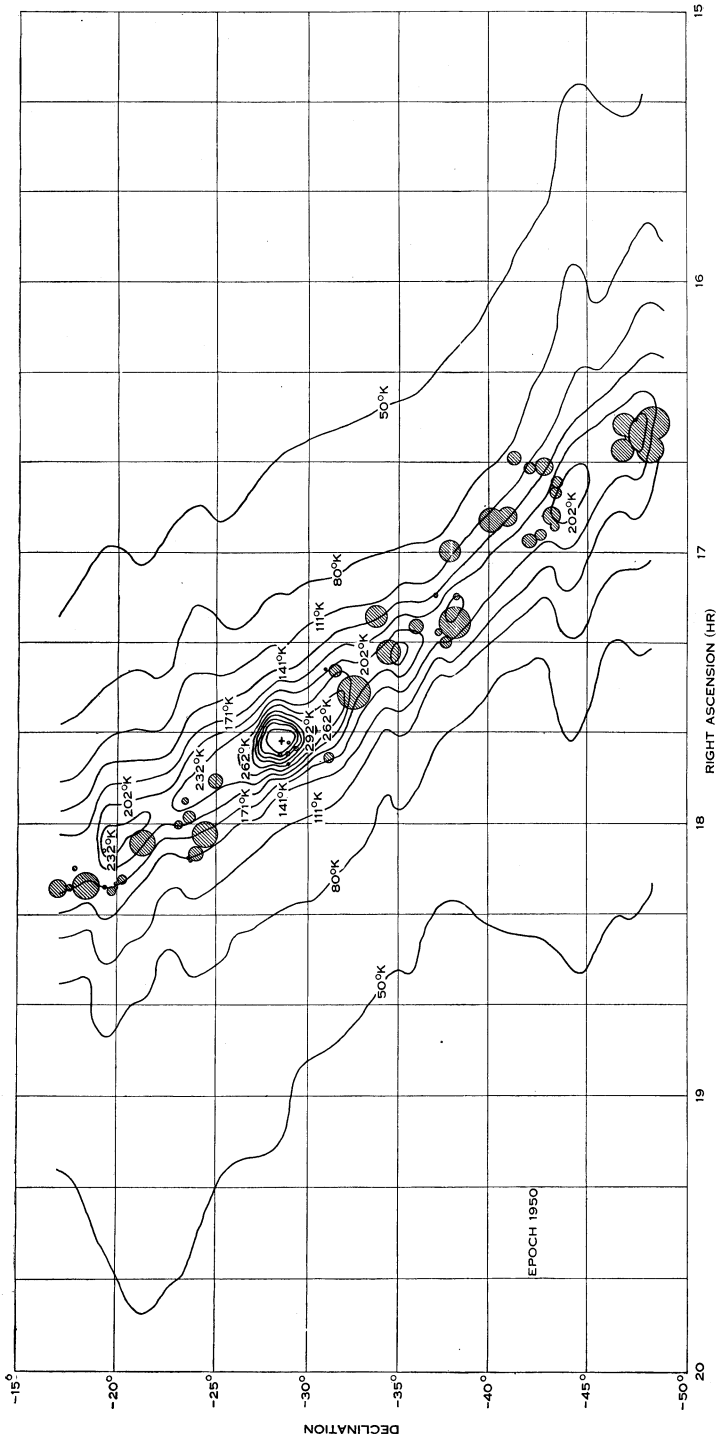

Fig. 2.—Contours of equivalent sky temperature at 400 Mc/s of central Milky Way plotted in celestial coordinates. The shaded circles represent optically observed emission regions.

eliminated. When the calibrating procedure described in Section III (*a*) had been carried out, it was found that one " Centaurus unit " represented an equivalent aerial temperature of 61 °K.

(*a*) *The Milky Way Contours*

Contours of aerial temperature were plotted directly in celestial coordinates (epoch 1950) and the final diagram is presented in Figure 2. Here the contour interval is 30·5 °K. The sky temperature along the first contour was checked at declinations −49°, −40°, −30°, and −20° by the absolute calibration technique referred to in Section IV (*b*).

For a general discussion the contours have been replotted in galactic coordinates. Precession corrections were applied to the celestial coordinates to transfer to epoch 1900 and the Lund Observatory Tables, based on the galactic pole R.A. 12 hr 40 min, Dec. +28° (1900), were used for the conversion. This plot appears in Figure 3, accompanied by the power diagram of the aerial.

The ability of the aerial to separate out some of the radio fine structure of the galaxy is now apparent. There are a number of intensity maxima representing discrete sources superimposed along the radio galactic plane. Particulars of these are given in Section VI (*b*). Studying what appear to be the contours of the background radiation, one can observe a fairly uniform increase in brightness from each side towards galactic longitude $l=328°$. It is estimated that here the background radiation from the Milky Way reaches a sky temperature of about 260 °K.

The diagram shows that almost all of the 400 Mc/s Milky Way in this zone is confined between $\pm 10°$ in galactic latitude. The mean width between half-power points is, in fact, only 5° over the observed range of l. The centre line of the marked concentration of radio brightness runs approximately along galactic latitude −1°. A fuller discussion of the shape of the observed contours will be given in a later paper.

(*b*) *The Galactic Nucleus Source*

The outstanding difference from previous radio surveys is the manner in which the prominent discrete source near the galactic centre emerges from the rest of the Milky Way. This source is probably the galactic nucleus itself. Its position is very close to the generally accepted position of the galactic centre, its coordinates being $l=327·9°$, $b=-1·0°$, with an estimated probable error in position of $\pm 0·2°$ in each case.

Statistical analysis of the counts of globular clusters, variable stars, and distant highly luminous objects such as planetary nebulae and novae, coupled with results obtained from measurements of galactic rotation and the motion of high velocity objects, place the direction of the galactic centre at 327° in galactic longitude with an uncertainty of about $\pm 1°$. The optical analysis of the region is, however, difficult because parts are heavily obscured, up to 8 magnitudes in some places, by clouds associated with the Ophiucus dark nebula. They include an area containing the very positions quoted above and as yet even infra-red observations have failed to locate the galactic nucleus.

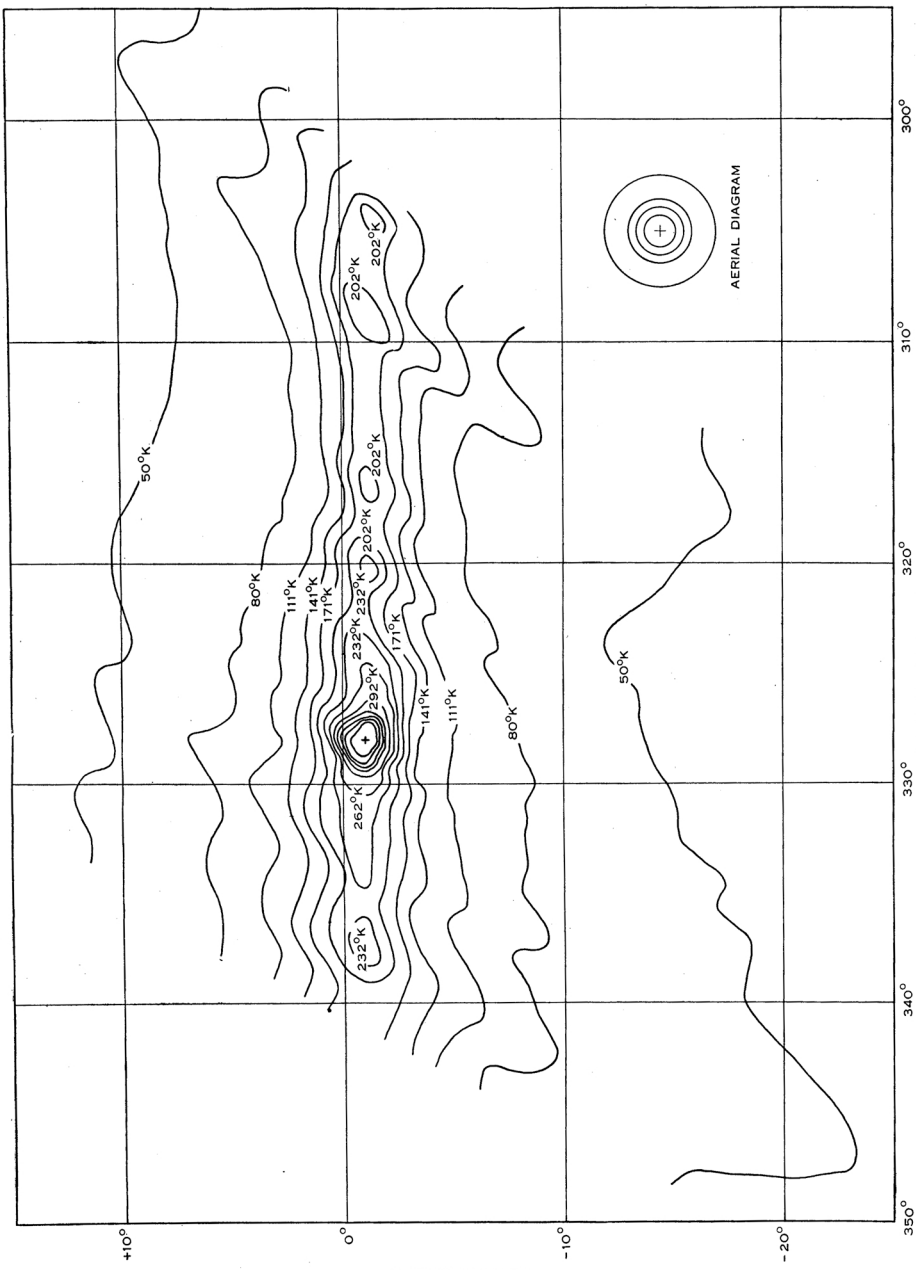

Fig. 3.—Contours of equivalent sky temperature at 400 Mc/s of central Milky Way plotted in galactic coordinates. At bottom right is a contour representation of the aerial power diagram. The circles represent the loci of the points at which received power drops to ¾, ½, ¼, and 0 (computed) of its value for the centre of the beam.

Until recently radio estimations of the position of the centre have been subject to as much uncertainty as have optical estimations. However, since this present survey was completed, a number of other high resolution observations have been made and in these there is agreement to within $\pm 0 \cdot 5$ min in Right Ascension and $\pm 0 \cdot 25°$ in declination. The details are summarized in Table 1.

TABLE 1

RECENT RADIO OBSERVATIONS OF PROBABLE GALACTIC NUCLEUS SOURCE

Frequency (Mc/s)	Position 1950		Flux Density ($W\ m^{-2}\ (c/s)^{-1}$)	Aerial Beam Width at Half Power	Observers
	R.A. (hr min)	Dec. (deg)			
250	17 43	—28·5	10×10^{-24}	1·2° in R.A. 17° in Dec.	Kraus, Ko, and Matt (1954)
400	17 42	—28·5	$16 \cdot 4 \times 10^{-24}$	2·1°	Present authors
760	17 42	—28·5	—	1·2°	Present authors (unpublished data)
1420	17 43	—28·75	17×10^{-24}	0·9°	Hagen, McClain, and Hepburn (1954)
3200	17 42·5	—29·0	$4 \cdot 8 \times 10^{-24}$	0·4° in R.A. 0·45° in Dec.	Haddock, Mayer, and Sloanaker (1954)

Knowledge of the size would be a most important factor in identifying this source with the galactic nucleus. Dr. Baade (private communication) has pointed out that for the Andromeda nebula M31, which is probably a close counterpart of our own galaxy, the semi-stellar nucleus has a diameter of 2·5 sec of arc. He therefore expects that the nucleus of our galaxy, which is 73 times closer, would have a diameter of 3 min of arc.

Up to the present the radio data on size is conflicting. In the 400 Mc/s survey (beam width 2°) the source appears as a point source when separated from the background. The separation was effected by studying profiles taken in several directions through the point of maximum intensity. It was estimated that the general Milky Way radiation rises to an equivalent sky temperature of 260 °K and that the " nucleus source " centred on the position of the maximum produces a further equivalent temperature of 180 °K. The authors also made some exploratory observations at 760 Mc/s with an aerial beam of 1·2° between half-power points but again failed to resolve the source. Moreover, from the information published by Haddock, Mayer, and Sloanaker (1954), it is inferred that the source was effectively a point source even to their 0·4° beam at 3200 Mc/s.

The confusion in size arises at the lower frequencies and is probably due to the use of interferometers and low resolution aerials to survey a region whose structure is so complex. The source, as observed at 100 Mc/s by the interferometers of Mills (1952) and Bolton, Stanley, and Slee (1954), would appear to be small in size. But Bolton *et al.* (1954), using a 6° pencil beam and an azimuth interferometer, report that the source is 12° by 2° to fifth-power points

with a strong central concentration. Shain and Higgins (1954) infer from scintillation observations at 18·3 Mc/s that the angular size to half power is 1° or greater.

Turning now to a discussion of the intensity of radiation from the nucleus source, the flux density is plotted against frequency for the determinations listed in Table 1 together with those at 18·3 Mc/s (Shain and Higgins 1954), 100 Mc/s (Mills 1952; Bolton, Stanley, and Slee 1954; Bolton *et al.* 1954) and 1210 Mc/s (Piddington and Minnett 1951). The order of the resolution in each case is indicated by the relative size of the symbols in Figure 4, circles

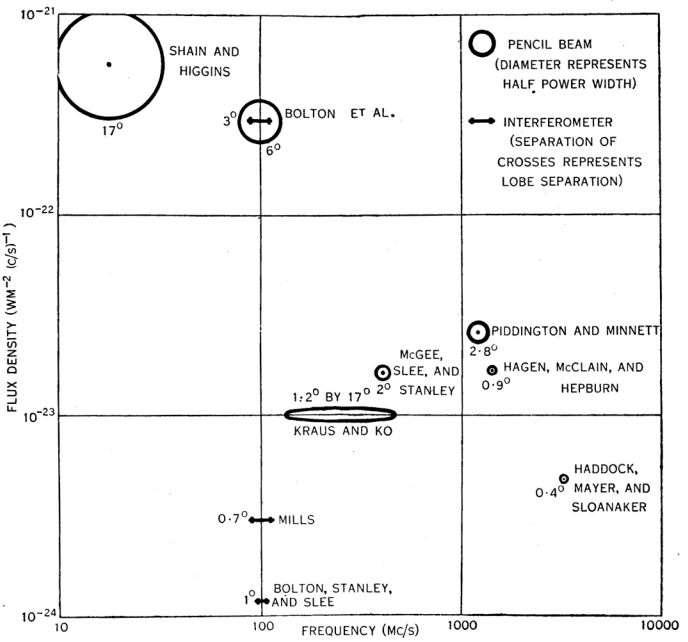

Fig. 4.—Radio-frequency radiation from the "galactic nucleus source".

being used to denote pencil-beam surveys and bars to denote interferometer surveys. A smooth spectrum curve could be drawn through the points above 250 Mc/s in frequency, especially since there are uncertainties of at least 20 per cent. in all the flux density values given. However, at 100 Mc/s, although the two interferometer points confirm one another within experimental error, the third point at this frequency, already a lower limit, has a flux density which is greater by a factor of 100. Under the circumstances no attempt is made to draw in a possible spectrum. It may be noted, though, on the one hand, if Mills and Bolton, Stanley, and Slee observed the same source as did Haddock, Mayer, and Sloanaker (unresolved with a 24′ beam), there is no reason to suspect that their values of flux density would be too low, and on the other, that Piddington and Minnett (1951) published for this source a smoothly descending spectrum which is similar to the first class of spectra discussed in Section VI (*c*). The latter spectrum is apparently supported by the point at 18·3 Mc/s.

Because of these discrepancies in size and intensity it appears possible that the nucleus source may have a complex structure with different parts of it displaying differing spectra. High resolution surveys at frequencies near 100 Mc/s and 20 Mc/s can make important contributions towards clearing up the present confusion.

(*c*) *Polarization Measurements at 400 Mc/s at Two Regions in the Milky Way*

Two regions were selected for some trial polarization measurements. They were centred on Dec. $-23{\cdot}5°$ and $-42{\cdot}75°$ at the radio galactic plane. The method was the simple one of twisting the primary dipole and reflector into a number of positions removed from the original and checking for any change in the recorded temperatures in any of the positions.

On each of five successive nights the following series of observations was taken : the usual Centaurus-A transit at Dec. $-42{\cdot}75°$ for relative calibration, the transit of the galaxy at the same declination, and the transit of the galaxy at Dec. $-23{\cdot}5°$. On the first night the equipment was set up using the normal east-west polarization of the dipole. On the second night the dipole was turned through 45° into a polarization approximately parallel to the galactic plane. On the third and fourth nights the dipole was placed in the north-south plane and in the direction perpendicular to the galactic plane respectively. The measurements were concluded with the dipole in its normal operating position as on the first night. Noise factor measurements indicated that the receiver sensitivity remained unchanged (to within 2 per cent.) over this period.

The recorded equivalent temperatures of each of the galactic regions exactly coincided on every run except No. 2 (polarization parallel to the galactic plane) when the temperature increased by 1 per cent. approximately. Thus, since reproduction of sensitivity could not be guaranteed to less than 2 per cent., it is concluded that at regions centred in R.A. 16 hr 54 min, Dec. $-42{\cdot}75°$ and R.A. 17 hr 55 min, Dec. $-23{\cdot}5°$ plane polarization of the radiation at 400 Mc/s is less than 2 per cent.

VI. Discrete Sources Observed at 400 Mc/s

The discrete radio sources observed in the course of this survey are set down in Table 2. The first two columns of the table give the reference number (assigned in order of increasing Right Ascension) and constellation in which the source is located. The next three columns give respectively the position in Right Ascension and declination for epoch 1950 and the estimated flux densities at 400 Mc/s for both planes of polarization in units of 10^{-24} W m^{-2} (c/s)$^{-1}$. Other authors' catalogue numbers of sources which appear to correspond are noted in the sixth column, and the final column contains remarks. The table is divided into two halves : sources 1–7 are isolated discrete sources lying outside the region covered by Figures 2 and 3, while sources 8–14 result from the analysis and composite plot of the Milky Way observations.

(*a*) *The Isolated Sources Nos.* 1–7

Since the survey was not designed for the searching out of discrete radio sources, there was not the same attention given to establishing their presence

TABLE 2

DISCRETE SOURCES OBSERVED AT 400 Mc/s

No.	Constellation	Position 1950		Estimated Flux Density at 400 Mc/s (Both Polarizations) (10^{-24} W m^{-2} (c/s)$^{-1}$)	Other Catalogue Nos.*	Remarks
		R.A. (hr min)	Dec. (deg)			
1	Fornax ..	03 20±1	−37·25±0·5	1·4	B_1A $B_2$10 MO3–3 SO3–4	Evidence of being slightly spread
2	Pictor	05 09±1 05 16±1	−42·75±0·5 −45·0±0·5	1·5	$B_2$22 MO5–4 SO5–4	Two maxima of approximate equal intensity; slightly spread
3	Puppis-Vela ..	08 24±2 08 35±2	−43·2±1 −45·1±1	1·5	B_1E $B_2$21 M08–4 B_1F S08–4	Point source on side of spread object, 15° by 15°, of maximum equivalent temperature 138 °K above cold sky. Flux density refers to point source
4	Antlia	09 59±1	−28·5±0·5	0·9	$B_2$102	One record only
5	Vela	10 41±1	−43·7±0·5	2·0	$B_2$50 M10–4	Elongated in galactic longitude
6	Centaurus ..	13 22·5	−42·75±0·1	6·0	B_1J $B_2$6 M13–4 H7 S13–4	Point source concentric with low intensity spread source. Flux density estimated for point source only
7	Lupus	15 04±1	−30·9±0·5	0·6	$B_2$110	

Sources 8–14 superimposed on galactic plane

8	Ara	16	34±1	—47·7±0·5	2·3	H19	Identified with H II region by Haddock, Mayer, and Sloanaker
9	Scorpius ..	17	04±1	—44·4±0·5	2·6	B_1K $B_2$114	Elongated in R.A. lying across galaxy
10	Scorpius ..	17	13±1	—38·1±0·5	3·3	M17–3 H13	Identified with H II region by Haddock, Mayer, and Sloanaker
11	Scorpius ..	17	23±1	—35·0±0·5	5·1	$B_2$17 H12	Identified with H II region by Haddock, Mayer, and Sloanaker
12	Sagittarius ..	17	42±1	—28·5±0·2	16·4	B_1L $B_2$68 M17–2B H5 S18–2	Probably galactic nucleus
13	Sagittarius ..	17	59±1	—21·5±0·5	2·8	M17–2A H10	Identified with H II region by Haddock, Mayer, and Sloanaker
14	Sagittarius ..	18	07±1	—19·6±0·5	3·6	$B_2$58	

* B_1, Bolton *et al.* (1954); B_2, Bolton, Stanley, and Slee (1954); M, Mills (1952); H, Haddock, Mayer, and Sloanaker (1954); S, Shain and Higgins (1954).

as was given to checking the features on the central region of the Milky Way. Thus quite a number of possible source observations have had to be omitted and sources 1–7 are those whose positions correspond fairly closely to previously observed sources. Some of the more important ones are discussed further.

Source No. 2 in Pictor

The observations on this source are interesting in that they reveal two maxima of approximately equal intensity. One, located in R.A. 05 hr 09 min, Dec. −42·75°, corresponds to the position of source 22 observed on the sea interferometer by Bolton, Stanley, and Slee (1954), while the other, in R.A. 05 hr 16 min, Dec. −45·0°, agrees approximately in declination although not in Right Ascension with Mills's source 05–4 (1952) observed with a Michelson-type interferometer. At 400 Mc/s the source is slightly wider in angular extent than the aerial diagram.

Source No. 3 in Puppis-Vela

Unfortunately only a restricted number of observations could be made on this region and good accuracy cannot be claimed for the positions given. At 400 Mc/s an extended source covers a large area of the sky approximately bounded by 08 hr 05 min and 09 hr 10 min in Right Ascension and by −38° and −48° in declination. It lies in the Hα emission region reported by Gum (1952), but there is no sign of correlation between the radio features and the stronger emission patches.

Superimposed on the general pattern of the observed radiation is a point source in R.A. 08 hr 24 min, Dec. −43·2°. This is most likely to be Puppis-A, identified by Baade and Minkowski (1954) with an unusual nebulosity in R.A. 08 hr 20 min, Dec. −42·8°. The extended source reaches a maximum equivalent temperature of 138 °K above the surrounding cold sky temperature in R.A. 08 hr 35 min, Dec. −45·1°. Neither of these radio positions is in good agreement with results by observers at other frequencies.

Source No. 6 in Centaurus

This is Centaurus-A, NGC5128, which has been extensively examined since its discovery and suggested identification by Bolton, Stanley, and Slee (1949). The R.A., 13 hr 22·5 min, was taken as a reference for this survey and the Dec., −42·75°, was that of the observed maximum brightness. The region was carefully observed and analysis of the records enabled the contour diagram of Figure 5 to be constructed. The contours are spaced at intervals of approximately 9 °K in equivalent aerial temperature and are plotted in celestial coordinates (epoch 1950). They have not been corrected for the effects of the aerial beam. The source appears as a spread object of approximate dimensions 5° by 3° to half power. Mills (1953) and Bolton *et al.* (1954) have referred to the fact that Centaurus-A consists of a point source and an associated spread object. In the present survey the point source is not separately distinguished.

(*b*) *The Central Milky Way Sources Nos.* 8–14

These sources are the maxima appearing along the surveyed zone of the Milky Way. The discrete source radiation merges into the general radiation

and it is difficult to decide where a separation should be made. In extracting a source from the " background " the following method was employed. The brightness contours in Figure 3 were imagined continued through the particular source under analysis according to the trend obtaining on either side, and points of equal excess brightness over them were joined to give a second system of contours, those of the " superimposed " source. With the exception of No. 9 all sources were unresolved by the 2° beam, and for flux density estimations they have been considered as point sources. All have been reported by other observers.

Observing at frequencies of 81·5 Mc/s and 210 Mc/s, Scheuer and Ryle (1953) discovered a narrow feature, 2° in angular width, superimposed on the background radiation between galactic longitudes 16°–338°. They attribute it

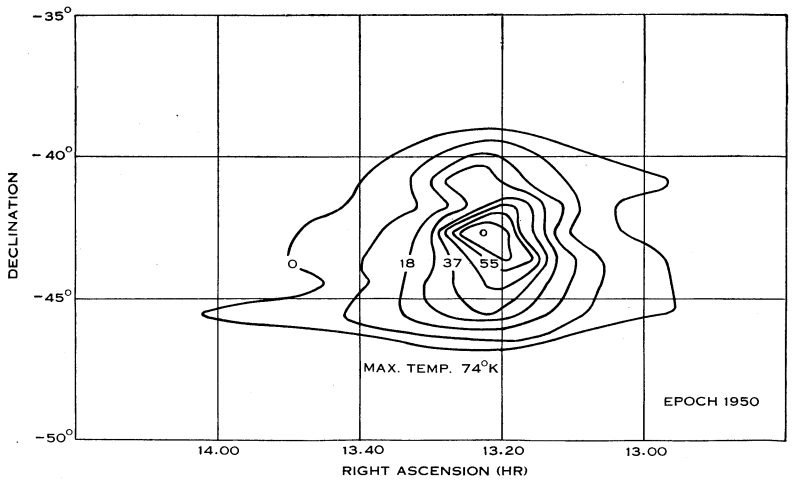

Fig. 5.—Contours of equivalent aerial temperature at 400 Mc/s of the discrete source Centaurus–A. Contour interval is 9·25 °K. (Not corrected for aerial beam.)

to H II emission. In order to test whether any correlation exists between the 400 Mc/s sources Nos. 8–14 and optically observed emission regions, a comparison is made in Figure 2. The shaded circles in the figure represent emission regions published by Sharpless (1953) in the zone of declinations north of Dec. —40°, and by Gum (1953) south of Dec. —35°. It will be noticed that the H II regions are closely grouped about the " 400 Mc/s galactic plane " but there is not a one-to-one correspondence with the radio sources. This may be due to insufficient aerial resolution. Haddock, Mayer, and Sloanaker (1954) with their 24′ beam width at 3200 Mc/s have positively identified the positions of four of the sources in Table 2 with H II emission regions. However, on the present evidence concerning the radiation spectrum, to be discussed in Section VI (*c*), it cannot be claimed that these sources are entirely due to thermal emission. More accurate spectrum information obtained by high resolution surveys at various frequencies is desirable for deciding whether or not the origin of this radiation is H II emission.

Source No. 9 in Scorpius

Reference to the contour diagrams of Figures 2 and 3 shows that source No. 9 is an extended line of increased brightness inclined to the galactic plane. But the fact that the line is approximately coincident with the parallel of declination −44° suggests the possibility of a spurious effect, e.g. an unaccounted change in receiver sensitivity over the observing period or an unusual aerial response when the mast is in this particular setting. No explanation of this nature was established. Several observations were taken on the central declination (−44·5°) and each time a similar pattern was obtained. Also closer spaced observations on either side of this declination merely confirmed the structure as plotted.

(*c*) *Discussion of the Radio-frequency Spectra*

All of the discrete sources under discussion have been observed by other workers at one or more different frequencies (see references in Table 2), and so the opportunity has been taken to examine trends in the radio-frequency spectra. In Figure 6 observed flux density in W m^{-2} $(c/s)^{-1}$ is plotted against frequency in Mc/s. Although the diagram suffers from the fact that in most cases there are too few points through which the spectrum curves are drawn it serves to illustrate the striking feature that the spectra of the 13 sources are divided into two distinct classes.

One class, characterized by a rapid decrease of flux density with frequency up to about 100 Mc/s and a subsequent gradual flattening out, is most fully represented by the spectrum for source No. 6, Centaurus-A. This curve is an extended version of the one published by Piddington and Minnett (1951). Closely following the same shape are the spectra of the well-known sources No. 1, Fornax-A; No. 2, Pictor-A; and No. 3, Puppis-A. Source No. 7 shows a similar curve over the range for which it is known.

The second class of spectra includes those of sources Nos. 4, 5, 9, 11, 13, and 14. The available data start at 100 Mc/s. The spectra exhibit an increase in flux density between 100 and 400 Mc/s followed by apparently the same type of gradual decrease towards high frequencies as in the first class. However, the increase may go past 400 Mc/s in the manner shown by the spectrum of No. 13. Sources Nos. 11 and 13 have been identified as H II regions by Haddock, Mayer, and Sloanaker (1954) while Nos. 9 and 14 may be associated with emission regions shown in Figure 2. At the low frequencies the spectra are similar to that of thermal emission from a cloud of ionized gas discussed, for example, by Piddington and Minnett (1952). Source No. 10 has a rather flat spectrum compared with either class but is identified with an H II region at 3200 Mc/s.

This division into two classes of observed spectra must correspond to an essential difference in the nature of the sources in the two groups. Two possible explanations are suggested, and in considering them one is reminded of the difficulties encountered in the nucleus source spectrum discussed in Section V (*b*).

One alternative is that a real difference in the spectra exists, thus giving evidence of a different mechanism in the production of radio-frequency radiation in each class of source.

GALACTIC SURVEY AT 400 MC/S

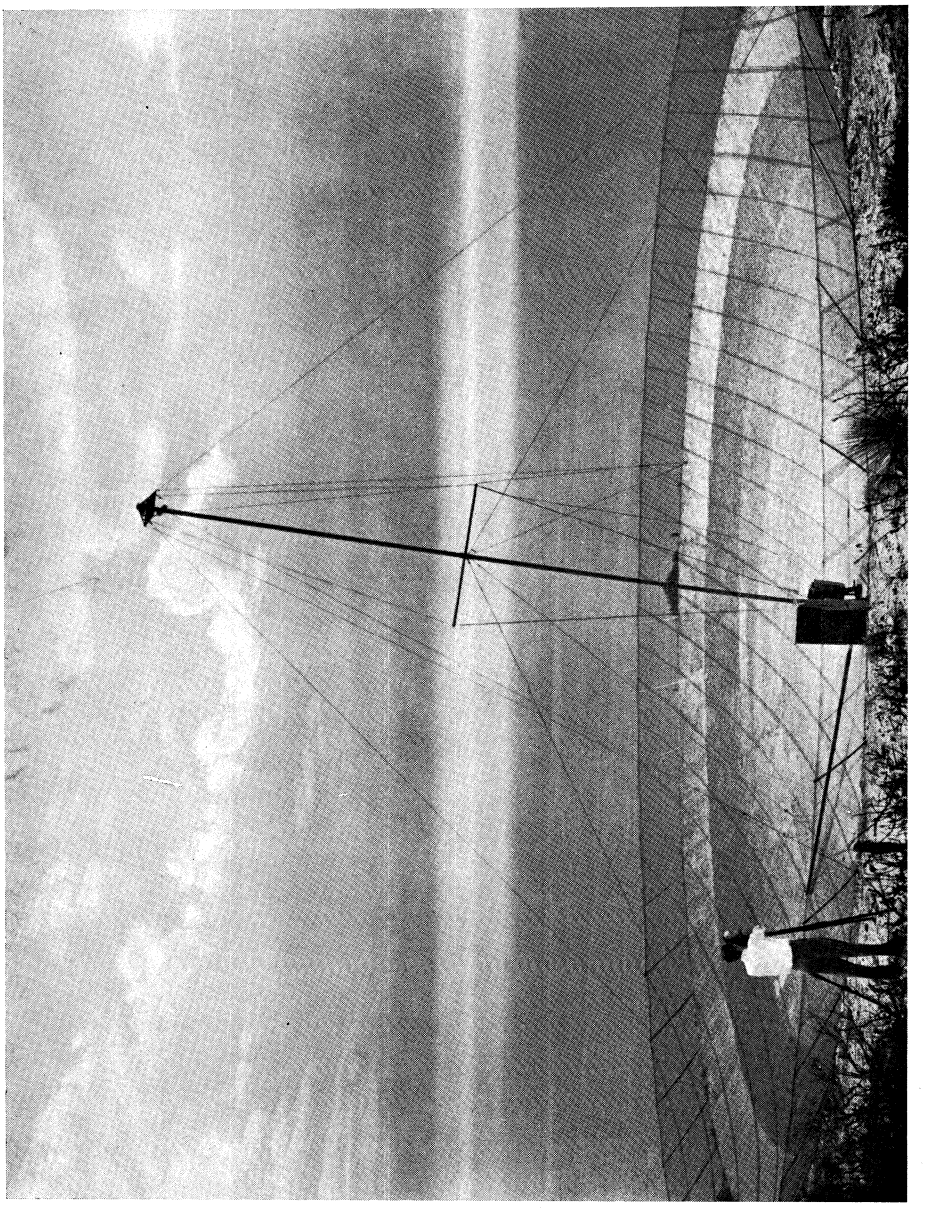

The 80-ft radio telescope.

The other, that the difference in spectra is only apparent, depends on the possibility that there has been an underestimation of flux densities at 100 Mc/s in the second class of sources. The observations at this frequency were made with interferometers of wide spacing and, if it happens that all these sources are systematically large, say, of the same order as the fringe spacing in angular

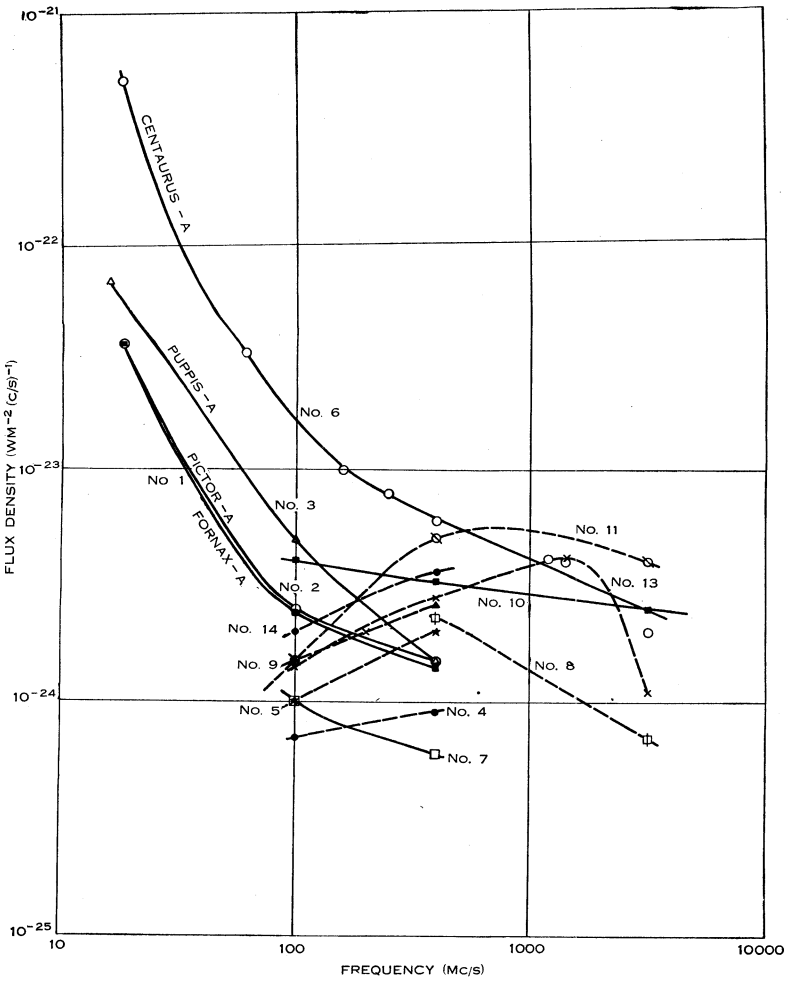

Fig. 6.—Radio-frequency spectra of 13 discrete radio sources.

size, then the interferometer observations would indicate intensities which were too low. The true flux densities may then be of such values that no division of spectra is warranted.

The question can be decided either when the true sizes of the second group have been established and all the flux densities are modified accordingly, or by observing the sources at similar resolving power to the present survey at frequencies near 100 Mc/s and lower. It is hoped that new instruments already

developed in this Laboratory, such as the Mills's " Cross " at 85 Mc/s, will soon supply the answer.

VII. Acknowledgments

The authors pay tribute to Mr. J. G. Bolton of this Laboratory, who initiated the survey and was always ready to assist in the work. They wish to thank their Group Leader, Dr. J. L. Pawsey, for his advice on calibration methods and most helpful criticism of the manuscript. Finally, the discussions and criticisms by the visiting astronomer, Martha E. Stahr-Carpenter, and by other colleagues are sincerely appreciated.

VIII. References

Baade, W., and Minkowski, R. (1954).—*Astrophys. J.* **119**: 206–14.
Bolton, J. G., Stanley, G. J., and Slee, O. B. (1949).—*Nature* **164**: 101.
Bolton, J. G., Stanley, G. J., and Slee, O. B. (1954).—*Aust. J. Phys.* **7**: 110–29.
Bolton, J. G., and Westfold, K. C. (1950).—*Aust. J. Sci. Res.* A **3**: 19–33.
Bolton, J. G., Westfold, K. C., Stanley, G. J., and Slee, O. B. (1954).—*Aust. J. Phys.* **7**: 96–109.
Brown, R. H., and Hazard, C. (1951).—*Mon. Not. R. Astr. Soc.* **111**: 357–67.
Gum, C. S. (1952).—*Observatory* **72**: 151–4.
Gum, C. S. (1953).—*Observatory* **73**: 123–5.
Haddock, F. T., Mayer, C. H., and Sloanaker, R. M. (1954).—*Nature* **174**: 176.
Hagen, J. P., McClain, E. F., and Hepburn, Nannielou (1954).—*Astr. J.* **59**: 323.
Kraus, J. D., Ko, H. C., and Matt, S. (1954).—*Astr. J.* **59**: 439–43.
McGee, R. X., and Bolton, J. G. (1954).—*Nature* **173**: 985.
Mills, B. Y. (1952).—*Aust. J. Sci. Res.* A **5**: 266–87.
Mills, B. Y. (1953).—*Aust. J. Phys.* **6**: 452–70.
Piddington, J. H., and Minnett, H. C. (1951).—*Aust. J. Sci. Res.* A **4**: 459–75.
Piddington, J. H., and Minnett, H. C. (1952).—*Aust. J. Sci. Res.* A **5**: 17–31.
Reber, G. (1944).—*Astrophys. J.* **100**: 279.
Reber, G. (1948).—*Proc. Inst. Radio Engrs., N.Y.* **36**: 1215–8.
Scheuer, P. A. G., and Ryle, M. (1953).—*Mon. Not. R. Astr. Soc.* **113**: 3–17.
Shain, C. A., and Higgins, C. S. (1954).—*Aust. J. Phys.* **7**: 130–49.
Sharpless, S. (1953).—*Astrophys. J.* **118**: 362–9.
Silver, S., and Pao, C. S. (1944).—M.I.T. Radiation Lab. Rep. 479.
Slater, J. C. (1942).—" Microwave Transmission." (McGraw-Hill: New York.)

Appendix I

Calculation of Aerial Temperature due to Thermal Emission from the Ground Surrounding the Paraboloidal Reflector

In Section III (*c*) equation (**4**) states that the temperature contribution T_g' at the feed and the ambient temperature T_0 are in the ratio of the power received by the feed from the surrounding medium other than the reflector itself to the power that would be received were the feed completely enclosed in a black body space at ambient temperature.

Equation (**4**) may be rewritten in the form

$$T_g' = T_0 \frac{\int_0^{\pi} \int_0^{2\pi} \{A_{||}(\theta, \varphi) P_{||}(\theta, \varphi) + A_{\perp}(\theta, \varphi) P_{\perp}(\theta, \varphi)\} \sin\theta \, d\theta \, d\varphi}{\int_0^{\pi} \int_0^{2\pi} P(\theta, \varphi) \sin\theta \, d\theta \, d\varphi}, \quad \ldots (5)$$

in which $A(\theta, \varphi)$ and $P(\theta, \varphi)$ have been split up into components parallel (subscript $||$) and perpendicular (subscript $\perp$) to the plane of incidence.

The observed power directivity pattern of the feed could be expressed analytically to a very close approximation by

$$P(\theta, \varphi)=(1-\sin^2\theta\cos^2\varphi)^3\sin^2(\tfrac{1}{2}\pi\cos\theta). \quad \ldots\ldots\ldots\ldots \quad (6)$$

Then

$$P_{||}(\theta, \varphi)=\sin^2(\tfrac{1}{2}\pi\cos\theta)\{(1-\sin^2\theta\cos^2\varphi)^3-\sin^2\varphi\}, \quad \ldots\ldots \quad (7)$$
$$P_{\perp}(\theta, \varphi)=\sin^2(\tfrac{1}{2}\pi\cos\theta)\sin^2\varphi.$$

Equation (5) now becomes

$$T_g'=T_0\frac{\int_0^{2\pi}\int_\theta^{\frac{1}{2}\pi}\sin^2(\frac{1}{2}\pi\cos\theta)\sin\theta\,(A_{||}+A_{\perp})\{(1-\sin^2\theta\cos^2\varphi)^3-\sin^2\varphi\}\mathrm{d}\theta\,\mathrm{d}\varphi}{\int_0^{2\pi}\int_0^{\frac{1}{2}\pi}\sin^2(\frac{1}{2}\pi\cos\theta)\sin\theta\,(1-\sin^2\theta\cos^2\varphi)^3\,\mathrm{d}\theta\mathrm{d}\varphi} \quad \ldots\ldots\ldots\ldots\ldots\ldots \quad (8)$$

The denominator of equation (8) was evaluated by analytical integration and for the numerator integration was performed analytically with respect to φ and numerically with respect to θ.

Absorption coefficients $A_{||}$ and $A_{\perp}$ were calculated from the usual Fresnel equations using the measured values of soil conductivity and dielectric constant.

Although integration is carried out over the full hemisphere bounded by the plane reflector, the power directivity term ensures that outside the ground over which the aerial pattern extends there is a negligible contribution to T_g'.